

INVESTIGATION OF COVALENT BINDING OF GOLD NANOPARTICLES TO CHITOSAN NANOFIBERS USING CELLULOSE AND HYALURONATE DIALDEHYDES

¹Lukáš MÜNSTER, ¹Alžběta DŮBRAVOVÁ, ¹Vítek HRBÁČEK, ¹Monika MUCHOVÁ,
^{1,2}Ivo KURITKA, ^{1,3}Petr HUMPOLÍČEK, ¹Jan VÍCHA

¹Centre of Polymer Systems, Tomas Bata University in Zlín, Zlín, Czech Republic, EU,
munster@utb.cz

²Department of Chemistry, Faculty of Technology, Tomas Bata University in Zlín, Zlín, Czech Republic, EU,
kuritka@utb.cz

³Department of Fat, Surfactant and Cosmetics Technology, Faculty of Technology, Tomas Bata University in
Zlín, Zlín, Czech Republic, EU, humpolicek@utb.cz

<https://doi.org/10.37904/nanocon.2024.5024>

Abstract

In this study, the reaction mechanisms of gold nanoparticles (AuNPs) synthesis using dialdehyde cellulose (DAC) and dialdehyde hyaluronate (DAH), and their covalent binding to chitosan nanofibers (CHITs), was investigated. The synthesis uses a redox reaction where dialdehyde polysaccharides are oxidized to dicarboxy polysaccharides and the gold salt precursor is reduced to elemental gold. The formation of the AuNPs-CHIT composite involves Schiff base chemistry, where reactive aldehyde groups of the polysaccharide shell around AuNPs react with chitosan's amine groups, forming pH-labile imine groups, which can be subsequently stabilized using reductive amination. FT-IR and XPS analyses were used to confirm the proposed reaction mechanisms. Next, the catalytic activity of AuNPs synthesized using DAC and DAH was evaluated for the reduction of 4-nitrophenol to 4-aminophenol with sodium borohydride. Rapid conversion rates and high turnover frequency were observed. The morphology and structure of the composites were characterized using transmission electron microscopy (TEM), scanning electron microscopy (SEM), and X-ray diffraction (XRD). These analyses confirmed the sub-10 nm size of the AuNPs and their uniform distribution on chitosan nanofibers. The findings confirm the proposed reaction mechanisms, showcase the morphology and catalytic activity of the prepared nanoparticles and highlight their potential industrial applications. The versatility of this method also opens avenues for further functionalization and broader applications of AuNPs in biomedical fields such as biosensors and drug delivery systems.

Keywords: Gold nanoparticles, dialdehyde cellulose, dialdehyde hyaluronate, chitosan nanofibers, catalysis

1. INTRODUCTION

Gold nanoparticles (AuNPs) are widely studied due to their unique optical, electronic, and catalytic properties, making them valuable for applications in catalysis, drug delivery, and biosensing [1–3]. However, ensuring stable binding of AuNPs to biocompatible substrates such as chitosan nanofibers remains a complex challenge [4]. Chitosan, a natural polymer known for its biocompatibility and antimicrobial properties, is an ideal candidate for such composite materials. This study investigates the covalent binding of AuNPs to chitosan nanofibers (CHITs) using dialdehyde cellulose (DAC) and dialdehyde hyaluronate (DAH) prepared employing simple periodate oxidation (POX), providing a robust method for composite synthesis with enhanced stability and functionality. Dialdehyde polysaccharides (DAPs), such as DAC and DAH, are valuable due to their triple role as reducing and stabilizing agents in nanoparticle synthesis, and as linker for covalent attachment to CHITs [5]. Derived from cellulose and hyaluronic acid, respectively, these materials contain reactive aldehyde (–CHO)

groups that readily form Schiff base linkages with the amine ($-\text{NH}_2$) groups of chitosan. This process creates covalent imine bonds, which can be further stabilized via reductive amination, ensuring stable attachment of AuNPs to chitosan nanofibers. This method effectively combines the catalytic properties of AuNPs with the functional benefits of substrates based on natural polymers.

In the synthesis represented in **Figure 1**, DAPs prepared by POX (part A) partially oxidize to dicarboxy polysaccharides, while the gold salt precursor is reduced to elemental gold (part B), forming AuNPs surrounded by a stabilizing polysaccharide shell. The $-\text{CHO}$ groups in the shell then bind covalently to chitosan's $-\text{NH}_2$ groups, ensuring robust nanoparticle attachment (part C). This approach provides stability in aqueous environments, a critical factor for many biomedical and industrial applications. Here, the reaction mechanisms of synthesis and covalent binding are studied and confirmed through Fourier-transform infrared spectroscopy (FT-IR) and X-ray photoelectron spectroscopy (XPS), which validates the reduction of Au^{3+} to Au^0 and partial oxidation of DAPs to dicarboxy polysaccharides (DCP), and the formation of imine/secondary amine bonds between $-\text{CHO}$ groups of AuNPs shell and chitosan's $-\text{NH}_2$ groups. Morphological analyses using transmission electron microscopy (TEM), scanning electron microscopy (SEM), and X-ray diffraction (XRD) revealed a uniform distribution of sub-10 nm AuNPs on the nanofiber surface, crucial for maximizing catalytic efficiency. The catalytic performance of the synthesized AuNPs was demonstrated in the reduction of 4-nitrophenol to 4-aminophenol, a common catalysis reaction [6], using UV-Vis analysis. The AuDAP-CHIT composites thus should also exhibit excellent catalytic performance suitable for industrial applications.

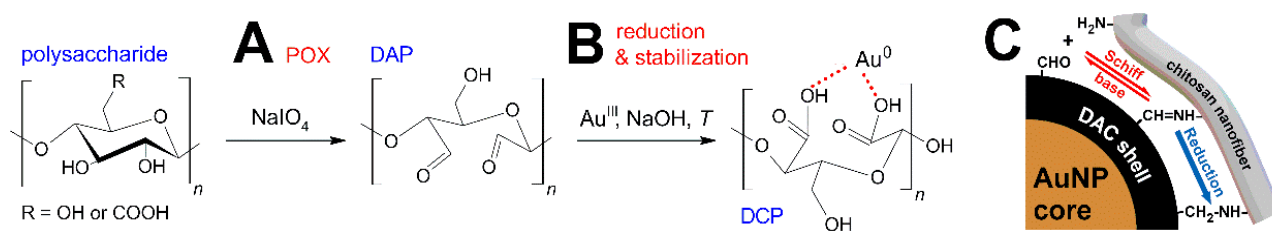


Figure 1 Scheme of polysaccharide POX to DAP (part A), subsequent reduction of gold(III) salt precursor and DAP partial oxidation to DCPs, and representation of covalent nanoparticle binding to CHITs via Schiff base chemistry and reductive amination forming AuDAP-CHIT composite (part C).

In conclusion, this study presents a versatile method for covalently binding AuNPs to chitosan nanofibers using DAPs. The composite materials show promising catalytic and biomedical potential, opening new possibilities for functionalized nanomaterials in applications such as biosensing and drug delivery.

2. EXPERIMENTAL PART

2.1 Materials

Cellulose SigmaCell type 20 (CELL, weight-average molecular weight $M_w = 76$ kDa, dispersity $\mathcal{D} = 4.7$, degree of polymerization $DP = 468$, Sigma Aldrich Co.), sodium hyaluronate (HA, $M_w = 396$ kDa, $\mathcal{D} = 5.9$, $DP = 987$) (Contipro, Czech Republic), sodium periodate (NaIO_4 , Penta, Czech Republic), gold(III) chloride trihydrate ($\text{HAuCl}_4 \cdot 3\text{H}_2\text{O}$, Sigma Aldrich Co.), medium molecular weight chitosan (75–85 % deacetylated, viscosity-average molecular weight $M_v = 190$ – 310 kDa, Sigma Aldrich Co.), acetic acid (CH_3COOH , Sigma Aldrich Co.) polyethylene oxide (PEO, $M_v = 600$ kDa, Sigma Aldrich Co.), sodium hydroxide (NaOH , Lachner, Czech Republic), hydrochloric acid (HCl , Penta, Czech Republic), sodium triacetoxyborohydride (STAB, Sigma Aldrich Co.), sodium borohydride (NaBH_4 , Sigma Aldrich Co.), and 4-nitrophenol (4-NP, Sigma Aldrich Co.) were used as received without further purification. Demineralized water (DEMI) of conductivity < 0.1 $\mu\text{S}/\text{cm}$ was used throughout the study.

2.2 Synthesis of DAPs

DAPs with a high degree of oxidation (*DO*) were prepared by POX of CELL and HA using a 1.2 molar excess of NaIO_4 at room temperature for 72 and 24 h, respectively [7]. Resulting DAC suspension was purified by 5 cycles of repeated centrifugation and mechanical homogenization, followed by solubilization procedure (i.e., stirring for 2 h at 80 °C under reflux in an oil bath [8]) and final centrifugation to obtain clear DAC solution. Both DAC and DAH solution were then dialyzed (dialysis tubing $MWCO = 14$ kDa) against DEMI for 72 h to remove oxidizing agent residues, flash-frozen, and lyophilized.

2.3 DAPs assisted AuNPs synthesis, AuDAP-CHIT composite preparation

DAPs were dissolved in water (0.6 wt%, $V = 9.4$ mL, shaken for 24 h at 40 °C), pH was adjusted to 7 using diluted NaOH solution, and DAPs solutions were placed in an oil bath heated to 90 °C for 15 min. Next, 100 μL of stock precursor solution (50 mg/mL of $\text{HauCl}_4 \cdot 3\text{H}_2\text{O}$ in DEMI) was added to hot DAPs solutions and vortexed for 5 s. Subsequently, 500 μL of 0.1 M NaOH solution was added to the reaction mixture, vortexed again, and immediately cooled under tap water. The formation of AuNPs took place instantly after NaOH addition. The cold AuNPs samples were transferred into dialysis tubing ($MWCO = 14$ kDa) and placed in acid dialysis medium (diluted HCl solution of pH 3.5) and dialyzed for 2 h. The resulting purified AuDAP samples, designated as AuDAC and AuDAH, were characterized by methods described below. AuDAPs samples were then covalently attached to CHITs (for details on CHITs preparation, see [5]). To each of AuDAP sample, with pH adjusted to 6.5, a 10 % w/v of washed and deprotonated CHIT was added and left to react for 3 h. The resulting AuDAC-CHIT and AuDAH-CHIT samples were thoroughly washed in DEMI, one half of each sample was left in unreduced state (without reductive amination, designated as AuDAP-CHIT_unred samples) and second half was placed in solution containing excess of STAB for 1 h to reduce imine groups formed between DAPs and CHIT, and washed in DEMI (designated as AuDAP-CHIT_red). Both types of samples were flash-frozen, lyophilized, and characterized.

2.4 Characterization of DAPs, AuDAPs, and AuDAPs-CHIT

All synthesized samples, including source materials, were characterized by FT-IR using a Nicolet 6700 spectrometer (Thermo Fisher Scientific, USA) equipped with a diamond crystal in ATR mode and 500–4,000 cm^{-1} wavenumber range. AuDAPs and AuDAPs-CHIT (unred and red) were characterized by XPS using an Axis Ultra DLD spectrometer equipped with a monochromatic $\text{Al K}\alpha$ ($h\nu = 1486.7$ eV) X-ray source (75 W, 5 mA, 15 kV), using base pressure of 2×10^{-8} , Kratos charge neutralizer system, and standard Shirley background. SEM and TEM analyses of prepared AuDAPs and AuDAPs-CHIT (red) were carried out on a Nova NanoSEM 450 scanning electron microscope (FEI, Czech Republic), and a JEM-2100 transmission microscope (JEOL, Japan), operated at a 5 and 160 kV accelerating voltages, respectively. AuDAPs-CHIT diffractograms were measured using a MiniFlex600 X-ray diffractometer (Rigaku, Japan) in the diffraction 2θ angle range 5–95° ($\text{CoK}\alpha$ $\lambda = 1.789$ Å, $\text{K}\beta$ line filter). Catalytic performance of AuDAPs was determined using 4-NP to 4-AP in NaBH_4 model catalytic reaction by monitoring decrease of 4-NP signal at 400 nm in time using a Lambda 1050 UV-Vis spectrometer (Perkin Elmer, USA) and calculations based on the work of Kozuch and Martin [9].

3. RESULTS AND DISCUSSION

The results of FT-IR analysis (**Figure 2**, part A) of all materials used and prepared in this study, as well as XPS analysis of the synthesized AuDAPs and AuDAPs-CHIT (red and unred) (**Figure 2**, parts B–M), are discussed below. After POX, both DAC and DAH IR spectra show typical band at 1730 cm^{-1} (–CHO groups), DAC spectrum shows also increase in absorbance at 885 cm^{-1} (hemiacetal structures). DAPs conjugation with CHITs form AuDAPs-CHIT (unred) samples, in which bands at 1730 (DAC's –CHO) and 1560 cm^{-1} (chitosan's – NH_2) disappears evidencing formation of imine bonds (1640 cm^{-1}). Subsequent imines reduction results in

formation of secondary amines manifested by band shoulder at 1065 cm^{-1} and weakening of absorbance at 1640 cm^{-1} , which is well in line with previously reported observations [10, 11].

XPS analysis of AuDAPs confirmed proposed reaction mechanisms of AuNPs synthesis and their covalent binding to CHITs. Both DAPs reduce gold salt as evidenced in XPS high-resolution Au 4f scans (**Figure 2**, parts B–C) while being partially oxidized ($-\text{CHO}$ to $-\text{COOH}$ groups) as noticeable from high-resolution C 1s scans, see **Figure 2**, parts D–E. The comparison of high-resolution C 1s and N 1s scans of unreduced and reduced AuDAPs-CHIT composites (**Figure 2**, parts F–I and J–M showing DAC- and DAH-based composites, respectively) exemplifies presence of imines after conjugation in both material types and their subsequent elimination (AuDAC-CHIT red) or decrease (AuDAH-CHIT red) accompanied by $-\text{CHO}$ group reduction as a result of the reductive amination.

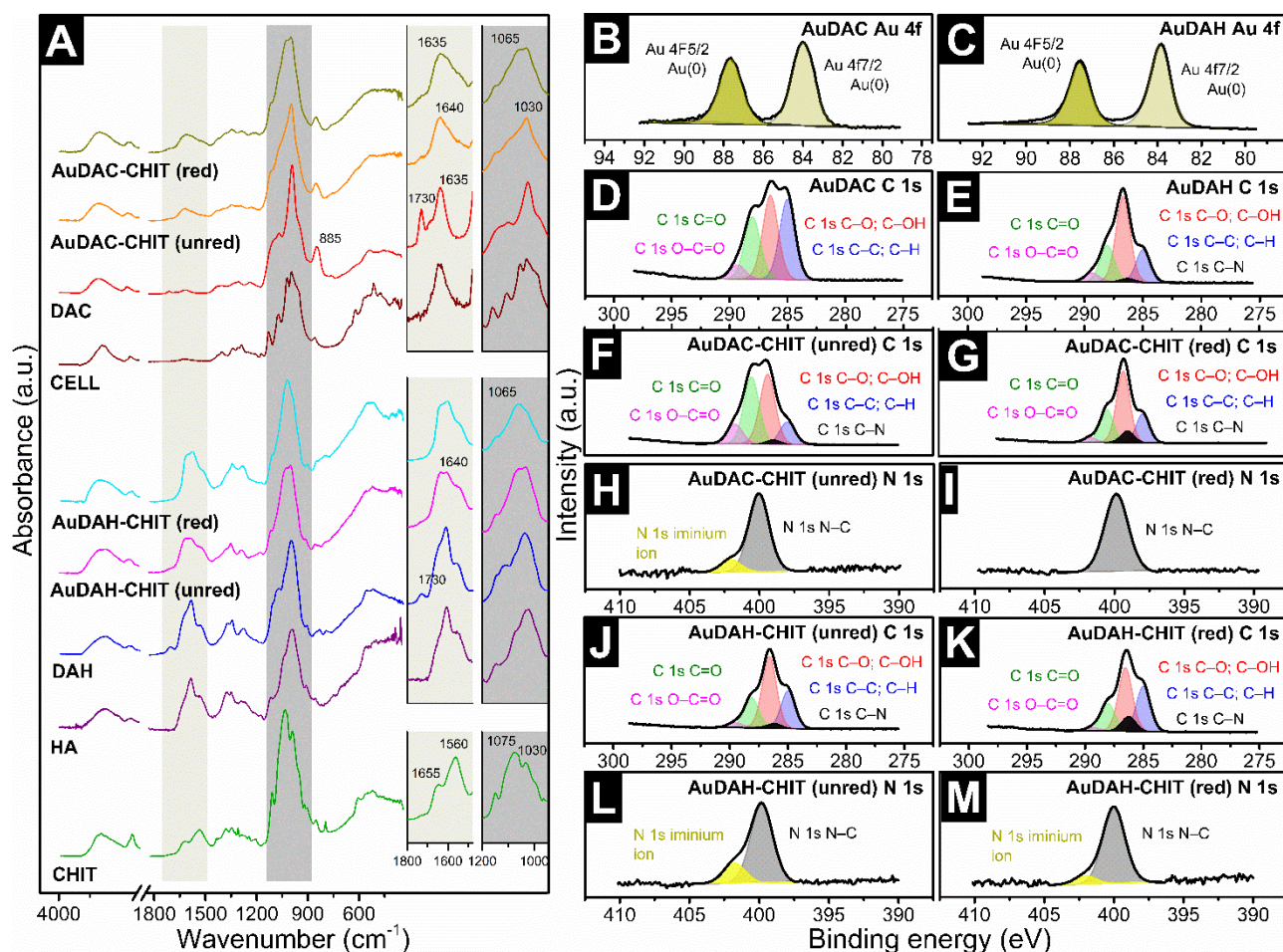


Figure 2 FT-IR analysis of used and resulting materials (part A). XPS analysis of all prepared composites including XPS high-resolution Au 4f, C 1s, and N 1s scans.

SEM and TEM analyses showed densely covered CHITs by covalently attached AuDAC (mostly spherical/polyhedral $6.2 \pm 2.4\text{ nm}$ nanoparticles) and AuDAH (triangular, bipyramidal, and spherical nanoparticles $9.8 \pm 4.1\text{ nm}$), although AuDAC-CHIT exhibit more uniform and densely surface-conjugated nanoparticles (**Figure 3**, left and center parts). The XRD analysis (**Figure 3**, right part) confirmed presence of Au in cubic crystalline lattice manifested by diffraction peaks at 44.64 (111), 52.04 (200), and 76.67 (220) 2θ $^\circ$. The loss of cellulose's crystallinity after POX, manifested by elimination of diffraction peak at 25.37 (-110) 2θ $^\circ$, is well in line with literature [12].

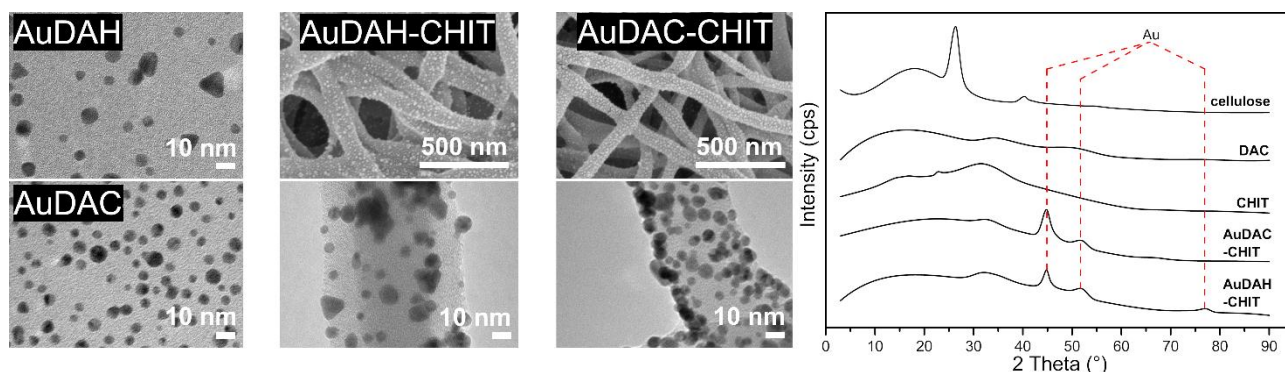


Figure 3 SEM and TEM analyses of the prepared AuDAPs and AuDAPs-CHIT composites (left and center parts, respectively), XRD analysis of used materials and resulting composites (right part).

Catalysis efficacy evaluation, performed using 4-NP to 4-AP reaction in presence of NaBH_4 (**Figure 4**, part A) and 2 μg of prepared AuDAPs samples, showed excellent performance with turn over frequencies (TOFs) between 27 and 29 min^{-1} (higher value for AuDAC) while maintaining relatively high catalysis reaction rate constant (k) between 0.65 and 0.7 min^{-1} (**Figure 4**, parts B and C). Catalytic performance was also for AuDAPs-CHIT composites and gold nanoparticles prepared using other DAPs, however, this topic will be discussed in more detail in our upcoming contribution.

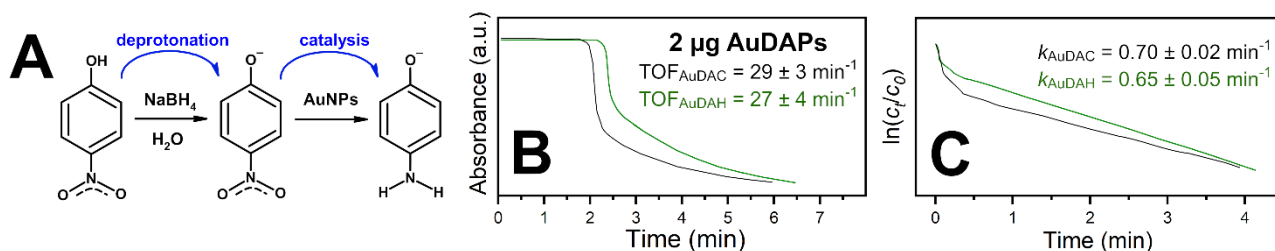


Figure 4 Catalysis efficacy evaluation using 4-NP to 4-AP (part A), calculated turn over frequency (TOF, part B) and catalysis reaction rate constant (k , part C) for both of the prepared AuDAPs samples.

4. CONCLUSION

In conclusion, this study successfully demonstrated the mechanisms of synthesis and covalent binding of gold nanoparticles (AuNPs) to chitosan nanofibers (CHITs) using dialdehyde cellulose (DAC) and dialdehyde hyaluronate (DAH) as both reducing and stabilizing agents and as linker. The synthesis was confirmed through various spectroscopic techniques, and the resulting AuNP-CHIT composites exhibited sub-10 nm nanoparticle size and uniform distribution. These composites demonstrated promising catalytic efficiency in the reduction of 4-nitrophenol, with excellent catalytic performance. The findings highlight the versatility and potential applications of these nanomaterials in biomedical fields such as drug delivery and biosensing.

ACKNOWLEDGEMENTS

L. Münster and J. Vícha gratefully acknowledge the Czech Science Foundation grant 23-07361S. M. Muchová and P. Humpolíček acknowledge the Centre of Polymer Systems Internal Development Project RP/CPS/2024-28/001 financed by the Ministry of Education, Youth, and Sports of the Czech Republic for infrastructural support. V. Hrbáček acknowledges the support by the Internal Grant Agency of TBU project no. IGA/CPS/2024/002. A. Důbravová and I. Kuřitka acknowledge the Centre of Polymer Systems Internal Development Project RP/CPS/2024-28/007 financed by the Ministry of Education, Youth and Sports of the Czech Republic for infrastructural support.

REFERENCES

- [1] KUSTOV, L. M. Catalytic properties of supported gold nanoparticles in organic syntheses. *Russian Chemical Bulletin*. 2013, vol. 62, no. 4, pp. 869–877.
- [2] COMENGE, J., C. SOTELO, F. ROMERO, O. GALLEGO, A. BARNADAS, T. G.-C. PARADA, F. DOMÍNGUEZ and V. F. PUNTES. Detoxifying Antitumoral Drugs via Nanoconjugation: The Case of Gold Nanoparticles and Cisplatin. *PLoS ONE*. 2012, vol. 7, no. 10, pp. e47562.
- [3] LEPINAY, S., A. STAFF, A. IANOUL and J. ALBERT. Improved detection limits of protein optical fiber biosensors coated with gold nanoparticles. *Biosensors and Bioelectronics*. 2014, vol. 52, pp. 337–344.
- [4] MATSUMOTO, M., K. KANEKO, M. HARA, M. MATSUI, K. MORITA and T. MARUYAMA. Covalent immobilization of gold nanoparticles on a plastic substrate and subsequent immobilization of biomolecules. *RSC Advances*. 2021, vol. 11, no. 38, pp. 23409–23417.
- [5] DŮBRAVOVÁ, A., M. MUCHOVÁ, D. ŠKODA, L. LOVECKÁ, L. ŠIMONÍKOVÁ, I. KUŘITKA, J. VÍCHA and L. MÜNSTER. Highly efficient affinity anchoring of gold nanoparticles on chitosan nanofibers via dialdehyde cellulose for reusable catalytic devices. *Carbohydrate Polymers*. 2024, vol. 323, pp. 121435.
- [6] MEJÍA, Y. R. and N. K. REDDY BOGIREDDY. Reduction of 4-nitrophenol using green-fabricated metal nanoparticles. *RSC Advances*. 2022, vol. 12, no. 29, pp. 18661–18675.
- [7] MUCHOVÁ, M., L. MÜNSTER, A. VÁVROVÁ, Z. CAPÁKOVÁ, I. KUŘITKA and J. VÍCHA. Comparison of dialdehyde polysaccharides as crosslinkers for hydrogels: The case of poly(vinyl alcohol). *Carbohydrate Polymers*. 2022, vol. 279, pp. 119022.
- [8] KIM, U.-J., M. WADA and S. KUGA. Solubilization of dialdehyde cellulose by hot water. *Carbohydrate Polymers*. 2004, vol. 56, no. 1, pp. 7–10.
- [9] KOZUCH, S. and J. M. L. MARTIN. “Turning Over” Definitions in Catalytic Cycles. *ACS Catalysis*. 2012, vol. 2, no. 12, pp. 2787–2794.
- [10] KIM, U.-J., H. J. KIM, J. W. CHOI, S. KIMURA and M. WADA. Cellulose-chitosan beads crosslinked by dialdehyde cellulose. *Cellulose*. 2017, vol. 24, no. 12, pp. 5517–5528.
- [11] GAO, C., S. WANG, B. LIU, S. YAO, Y. DAI, L. ZHOU, C. QIN and P. FATEHI. Sustainable Chitosan-Dialdehyde Cellulose Nanocrystal Film. *Materials*. 2021, vol. 14, no. 19, pp. 5851.
- [12] KIM, U.-J., S. KUGA, M. WADA, T. OKANO and T. KONDO. Periodate oxidation of crystalline cellulose. *Biomacromolecules*. 2000, vol. 1, no. 3, pp. 488–492.